First evidence of an intercalar bone in the braincase of "palaeonisciform" actinopterygians, with a virtual reconstruction of a new braincase of *Lawrenciella* Poplin, 1984 from the Carboniferous of Oklahoma

Alan PRADEL
CR2P UMR 7207 (MNHN, CNRS, UPMC, Sorbonne Universités),
Département Histoire de la Terre, Muséum national d'Histoire naturelle,
case postale 38, 57 rue Cuvier, F-75231 Paris cedex 05 (France)
and Department of Vertebrate Paleontology,
American Museum of Natural History, New York (United States)
alan.pradel@mnhn.fr

John G. MAISEY
Department of Vertebrate Paleontology,
American Museum of Natural History, New York (United States)
maisey@amnh.org

Royal H. MAPES
Department of Invertebrate Paleontology,
American Museum of Natural History, New York (United States)
mapes@ohio.edu

Isabelle KRUTA
CR2P UMR 7207 (MNHN, CNRS, UPMC, Sorbonne Universités),
Université Pierre et Marie Curie Paris VI, case 104,
4 place Jussieu, Paris cedex 05 (France)
and Department of Invertebrate Paleontology,
American Museum of Natural History, New York (United States)
isabelle.kruta@upmc.fr

Published on 30 December 2016

urn:lsid:zoobank.org:pub:4ABF9491-B7FC-42EE-88D2-636127350F40

Pradel A., Maisey J. G., Mapes R. H. & Kruta I. 2016. — First evidence of an intercalar bone in the braincase of "palaeonisciform" actinopterygians, with a virtual reconstruction of a new braincase of *Lawrenciella* Poplin, 1984 from the Carboniferous of Oklahoma. *Geodiversitas* 38 (4): 489-504. https://doi.org/10.5252/g2016n4a2

ABSTRACT
We describe here a new *Lawrenciella* Poplin, 1984 specimen from the Upper Carboniferous (Missourian, Pennsylvanian) from Oklahoma, USA. This specimen is three dimensionnally preserved in a phosphatic nodule. It was scanned by X-Ray microtomography. The neurocranium shows some morphological differences from *Lawrenciella schaefferi* Poplin, 1984, which might represent individual variability. The parasphenoid and a pair of intercalar bones are associated with the braincase. The presence of intercalars as an anterior extension covering the otico-occipital fissure have not been yet documented in "paleonisciforms" and may have a phylogenetic signal. A discussion about the evolutionary role of such intercalars in the closure of the otico-occipital fissure in modern actinopterygians is provided.

KEY WORDS
Paleozoic
actinopterygians,
intercalar,
braincase,
X-ray microtomography.

RÉSUMÉ
Découverte d'un os intercalaire dans le neurocrâne d'un actinoptérygien « paléonisciforme », avec une reconstitution virtuelle d'un nouveau neurocrâne de Lawrenciella *Poplin, 1984 du Carbonifère de l'Oklahoma (États-Unis).*
Nous décrivons ici un nouveau spécimen de *Lawrenciella* Poplin, 1984 du Carbonifère supérieur (Missourien, Pennsylvanien) de l'Oklahoma des Etats-Unis d'Amérique. Ce spécimen est préservé en trois dimensions dans un nodule phosphaté et a été scanné par microtomographie aux rayons X. Le neurocrâne présente quelques différences morphologiques par rapport à *Lawrenciella schaefferi* Poplin, 1984 qui peuvent traduire une variation individuelle pour ce taxon. Le parashénoïde ainsi qu'une paire d'intercalaires sont associés au neurocrâne. La présence d'intercalaires sous forme d'une excroissance antérieure recouvrant la fissure otico-occipitale n'avait encore jamais été documentée chez des « paleonisciformes » et pourrait comporter un signal phylogénétique. Une discussion sur le rôle évolutif des intercalaires dans la fermeture de la fissure otico-occipitale chez les actinoptérygiens modernes est également apportée.

MOTS CLÉS
Actinoptérygiens paléozoïques, intercalaires, neurocrâne, microtomographie à rayons X.

INTRODUCTION

Recent ray-finned fishes (actinopterygians) represent the majority of living vertebrate species and biomass (Faircloth *et al.* 2013). They comprise four major groups, the Polypteriformes, Chondrostei, Holostei and Teleostei (Grande 2010; Faircloth *et al.* 2013; Sallan 2014) that diverged before the end of the Paleozoic. Interrelationships of Paleozoic actinopterygian clades, notably taxa commonly assigned to the "palaeonisciforms", are still under discussion. Much of this phylogenetic uncertainty stems from a lack of well preserved, suitably informative fossils. Most Paleozoic actinopterygians are preserved in a flattened state and are often incomplete, so that endo- and exoskeletal information are incomplete. More rarely, three-dimensional braincases are preserved, providing a rich source of morphological and phylogenetical information (Poplin 1974, 1984; Gardiner 1984; Gardiner *et al.* 1996; Coates 1999; Hamel & Poplin 2008; Giles & Friedman 2014; Giles *et al.* 2015a, b). In the last ten years, the advances in non-destructive techniques of observation, such as computed X-ray microtomography (XR-µCT scan) and X-ray synchrotron microtomography (SR-µCT scan), have allowed the detailed study of both external and internal anatomy of number of Paleozoic jawed vertebrates braincases, providing anatomical information that is otherwise almost inaccessible (Maisey 2005, 2007; Hamel & Poplin 2008; Lane 2010; Maisey & Lane 2010; Pradel *et al.* 2009a, b, 2011, 2014; Pradel 2010; Giles & Friedman 2014; Dupret *et al.* 2014; Giles *et al.* 2015a, b).

Here we study a rare, 3D preserved braincase fortuitously associated with some dermal bones of a Paleozoic actinopterygian from the Late Carboniferous (Missourian, Upper Pennsylvanian) of Oklahoma, USA, by means of XR-µCT scan. This specimen is very similar to slightly younger isolated braincases belonging to *Lawrenciella schaefferi* Poplin, 1984 (Poplin 1984; Hamel & Poplin 2008) from the late Virgilian (Upper Pennsylvanian) of Kansas, USA. However, it possesses distinct paired intercalar bones arising from the cranio-spinal process and bridging the otico-occipital fissure, as in the Mesozoic caturids, pholidophoris, leptolepids, *Amia* Linnaeus, 1766 and modern teleosts (Schaeffer 1971; Patterson 1975) that were not previously documented in any "palaeonisciform".

MATERIAL AND METHODS

The specimen AMNH FF 20852 is preserved in an unbroken phosphatic nodule (Fig. 1) that was collected from the Coffeyville Formation (Pennsylvanian, Missourian, *c.* 307 Myr), at a road cut in Tulsa County, Oklahoma, USA (Center of NW sec. 2., T. 18N, R. 12E, Sapulpa North 7 1/2 Quadrangle).

The nodule has been scanned by µCT scan at the Microscopy and Imaging Facility of the American Museum of National History (AMNH), New York, USA, using a Phoenix V | tomex | X s 240 CT Scanner. Scan parameters were as follows: 185 kv x-ray tube with voxel size of 28 µm; 0.1 mm copper filter.

The segmentation and 3D rendering of the specimen were performed with MIMICS 15.01 64-bit software.

ANATOMICAL ABBREVIATIONS

a.fb	anterior fossa bridgei;
ant.amp	anterior ampulla;
ant.asc.p	anterior ascending process;
ant.c.v	foramen or canal for the anterior cerebral vein;
ant.d.fon	anterior dorsal fontanelle;
ant.s.c	anterior semicircular canal;
ao.c	aortic canal or its openings;
a.octl	area octavolateralis;
art.1.i	articular facet for the first infrapharyngobranchial;
art.1.s	articular facet for the first suprapharyngobranchial;
aur	cerebellar auricle;
bhc	bucco-hypophyseal canal or its ventral opening;
b.oc.a	foramen or canals for branches of the occipital artery;
b.p	basipterygoid process;
bsph	pars basisphenoidea;
c.c	crus commune;
c.r.d	canal for branches of the superficial ophthalmic nerves;

cr.csp	crista above the posterior semicircular canal;
cr.o	crista occipitalis;
crs.p	cranio-spinal process;
d.ant.my	dorsal anterior myodome;
die	diencephalon;
epi	epiphyseal part of the anterior dorsal fontanelle;
epi.a	foramen for epibranchial arteries;
epi III, IV	epibranchial arteries III and IV;
e.hy.a	efferent hyoid artery foramen;
e.ps.a	efferent pseudobranchial artery or its groove or notch;
f.hm	articular facet for the hyomandibular;
f.m	foramen magnum;
f.ram.dors	foramina for branches of the ramus ophthalmicus superficialis trigemini, the ramus ophthalmicus lateralis and vessels;
f.r.d	foramina for branches of the superficial ophthalmic nerves;
g.e.hy.a	groove for the efferent hyoid artery;
h.amp	horizontal ampulla;
h.s.c	horizontal semicircular canal;
hy.o.a	hyo-opercular artery;
int	intercalar bone;
int.car	internal carotid artery, or its foramen, groove or notch;
iorb.s	interorbital septum;
j.c	jugular canal or its anterior opening;
j.d	jugular depression;
l.ao	lateral aorta, or its groove;
l.c	lateral commissure;
l.cr.c	lateral cranial canal;
l.d.v	longitudinal dorsal vein;
l.ex.oc	dorso-lateral prominence of the occipital ossification;
l.r	lateral ridges;
l.st.a	longitudinally striated area overhanging the posterior dorsal fontanelle;
md.c.v	middle cerebral vein;
m.r	median ridge;
my	posterior myodome;
mye	myelencephalon;
not	notochordal canal, or its posterior opening;
oc.a	occipital artery, or its foramen and groove;
oims1, oims2	areas of insertion of the first and second intermuscular septa;
olf.b	olfactive bulbs;
oph.a	ophthalmic artery foramen, or canal;
opt.a	optic artery;
opt.l	optic lobe;
o.rec.m	insertion of the superior, inferior, and internal recti muscles;
ot.oc.f	otico-occipital fissure;
pal.a	palatine artery, or grooves for the palatine artery and nerve;
p.fb	posterior fossa bridgei;
pit	hypophyseal recess;
pit.fon	pituitary fontanelle;
pit.v	pituitary vein, or its groove;
po.p	postorbital process;
post.amp	posterior ampulla;
post.asc.p	posterior ascending process;
post.d.fon	posterior dorsal fontanelle;
post.s.c	posterior semicircular canal;
pr.b	prootic bridge;
p.spi.c	prespiracular canal;
p.spi.f	prespiracular fossa;
r.gass.lat.g	recessus for the gasserian and lateralis ganglia;
r.gen.g	recessus for the geniculate ganglion;
sac	saccular recess;
spic	spiracular canal, or its opening;
spi.g	spiracular groove;

Fig. 1. — Photograph of the nodule that houses the specimen studied here (AMNH FF 20852). Scale bar: 5 mm.

spio	spinooccipital nerve, or its foramen;
s.s	supraorbital shelf;
s.su	sinus superior;
s.vasc	space for the saccus vasculosus;
tel	telencephalon;
tr.f.ch	trigeminofacialis chamber;
utr	utricular recess;
v.font	vestibular fontanelle;
v.ot.f	ventral otic fissure;
zy	zygal plate;
I	canal or foramen for the olfactive nerves;
II	canal or foramen for the optic nerves;
III	canal or foramina for the oculomotor nerve;
IV	canal or foramen for the trochlear nerve;
V_o	canal or foramen for the profundus nerve;
V+VII lat	foramen or canal for the trigeminal and the lateralis trunk of the facial nerve;
VI_1, VI_2	foramina or canals for the abducens nerve;
VII	canal for the facial nerve;
VIIhy	hyomandibular trunk of the facial nerve;
VIIop	opercular branch of the facial nerve;
VIIpal	palatine nerve, or its canal or foramen;
IX	glossopharyngeal nerve, or its canal or foramen;
IXst	supratemporal branch of the glossopharyngeal nerve, or its foramen or groove;
X	vagus nerve, or its foramen.

SYSTEMATIC PALEONTOLOGY

Superclass OSTEICHTHYES Huxley, 1880
Class ACTINOPTERYGII Cope, 1887
Infraclass ACTINOPTERI Cope, 1871

Genus *Lawrenciella* Poplin, 1984

Type species. — *Lawrenciella schaefferi* Poplin, 1984 by original designation.

Lawrenciella sp.

Examined material. — AMNH FF 20852.

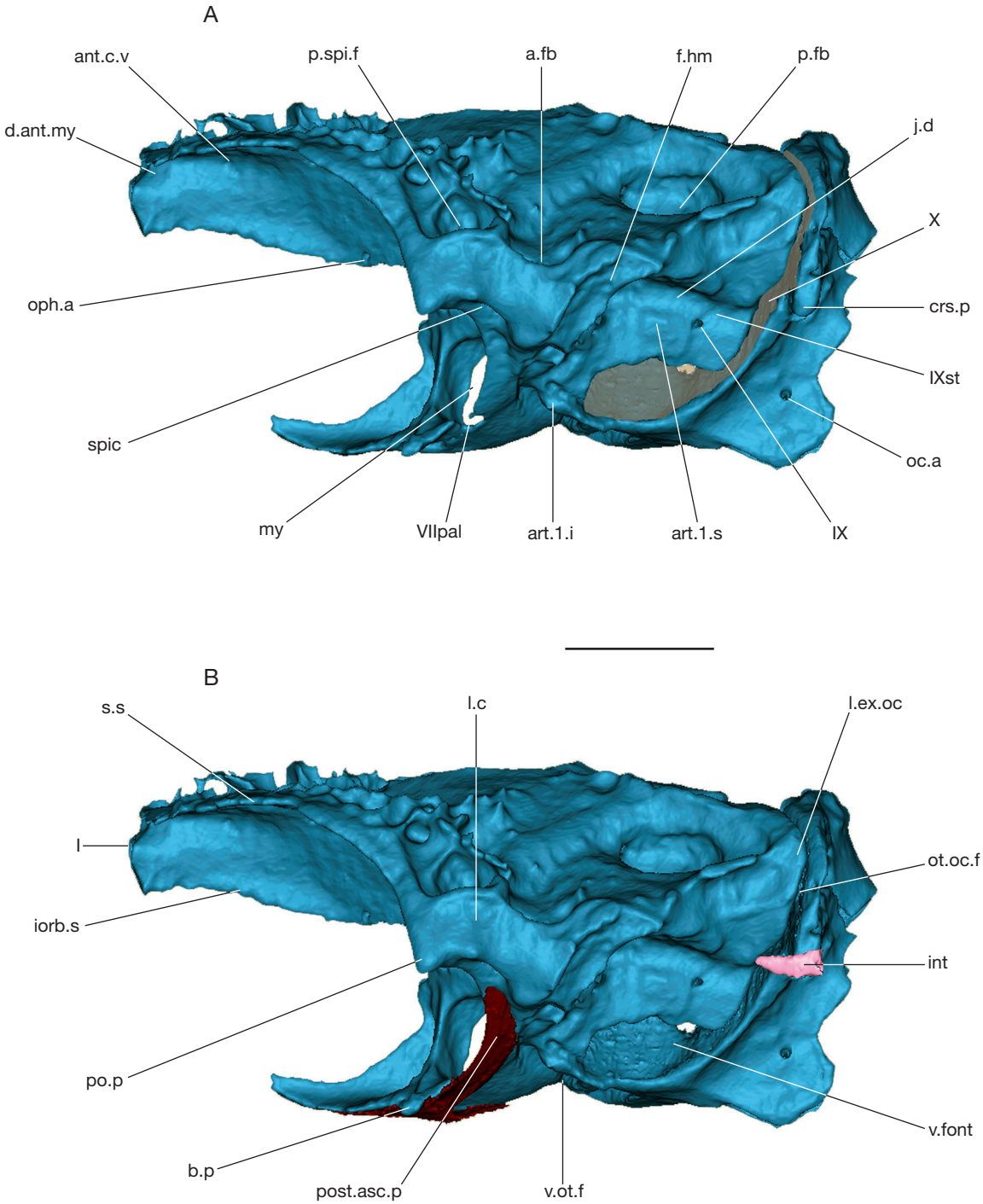

Fig. 2. — Surface rendering generated from CT Scan slices of the left lateral surface of AMNH FF 20852: **A**, braincase (**blue**); **B**, braincase (**blue**) and associated bones (intercalar in pink; parasphenoid in red). **Grey area**, not perichondrally lined surface. Abbreviations: see Material and methods. Scale bar: 5 mm.

Characters

Lawrenciella sp. shares with *Lawrenciella schaefferi* the following diagnostic features of the genus and species (Hamel & Poplin 2008): presence of paired prespiracular fossae; anterior edge of the posterior dorsal fontanelle overhung by the tip of a medial bony prominence; ventral otic fissure separated from the vestibular fontanelle by a bony bridge; posterior myodome unpaired, large and without a ventral fenestra; lateral cranial canals bulging blindly through the loop of the posterior semicircular canals; dorsal aortic canal extending from the occipital face to a level just behind the ventral otic fissure, with a single median bilobate anterior foramen for the lateral dorsal aortae and, at mid length, with a median opening for efferent branchial arteries; notochordal canal ending blindly, without reaching the ventral otic fissure; presence of wide and irregular intracranial cavities lateral to each jugular canal; absence of a cerebellar corpus at the metencephalic region of the braincast; optic

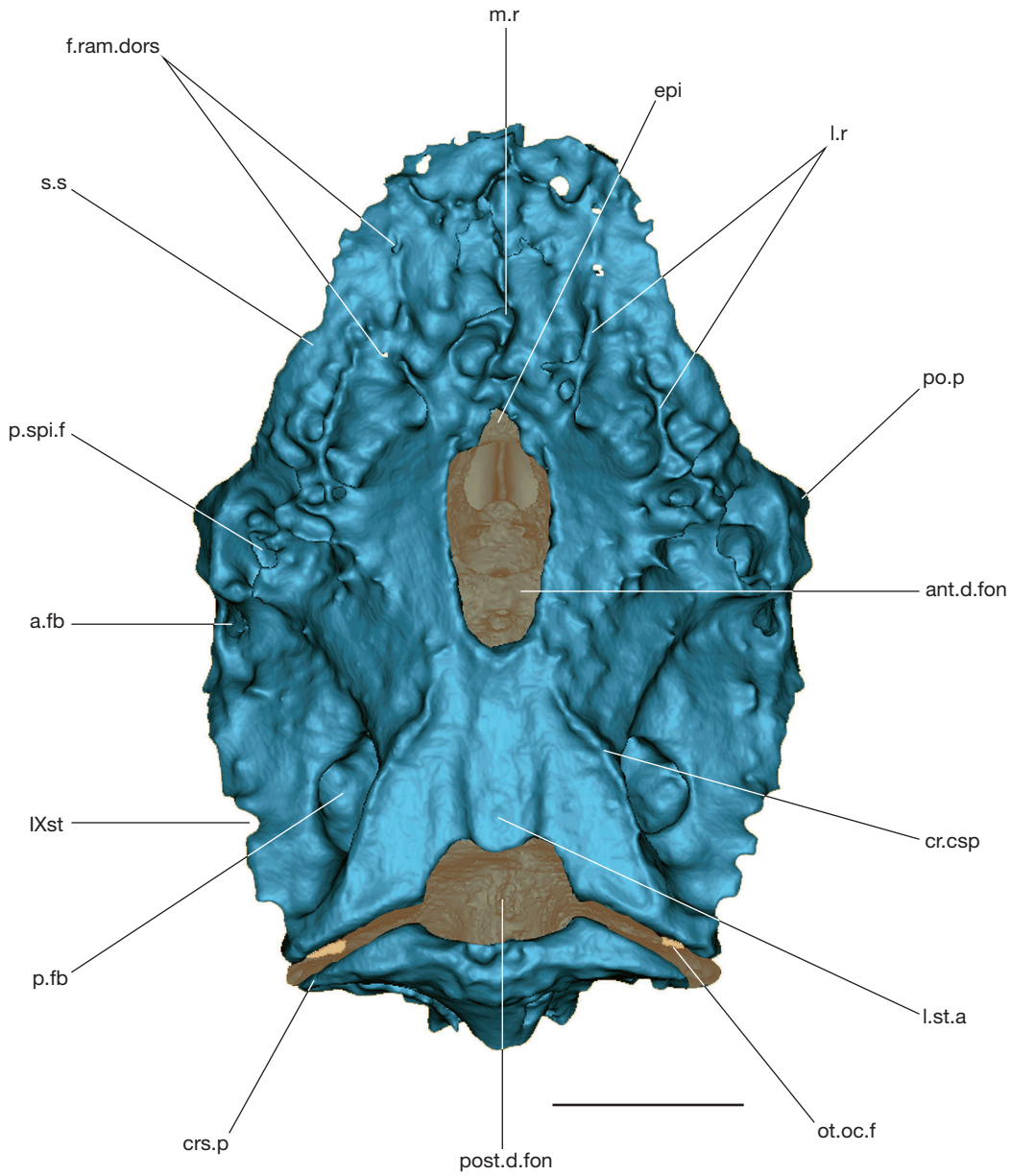

FIG. 3. — Surface rendering generated from CT Scan slices of the dorsal surface of the braincase (**blue**) of AMNH FF 20852. **Grey area**, not perichondrally lined surface. Abbreviations: see Material and methods. Scale bar: 5 mm.

nerves leaving the cranial cavity through a single foramen; canal for the lateralis nerve incompletely separated from the trigeminal canal; profundus nerve canal independent from the trigeminofacialis complex; absence of a distinct canal for the superficial ophthalmic branch of the facial nerve in the posterior wall of the orbit; no palatine foramen in the floor of the jugular canal; internal carotids penetrating into the braincase through two separate canals; anterior cerebral veins leaving the endocranial cavity at the level of the diencephalon, the left one always through an independent bony canal toward the left orbital cavity; inner wall of the unpaired posterior myodome with lateral deep grooves for the pituitary veins; parasphenoid with very short anterior ascending processes, and large and long posterior ascending processes reaching the spiracular canals.

Lawrenciella sp. differs from *Lawrenciella schaefferi* diagnosis in its smaller size (see below); the presence of posterior fossa bridgei with intramural diverticuli; no intracranial ossicles; absence of paired anterior myodomes for nonocular muscles below the olfactory nerve canal; absence of single median anterior myodome for ocular muscles; parasphenoid not extending to the ventral otic fissure posteriorly. However, we prefer not to erect a new species based on such differences, because their systematic significance is uncertain.

DESCRIPTION

General features

The braincase is fully ossified, except for the ethmoid region where the nasal capsules are not preserved. As many other "palaeonisciformes", the endocranium shows no sutures. The ethmoidal,

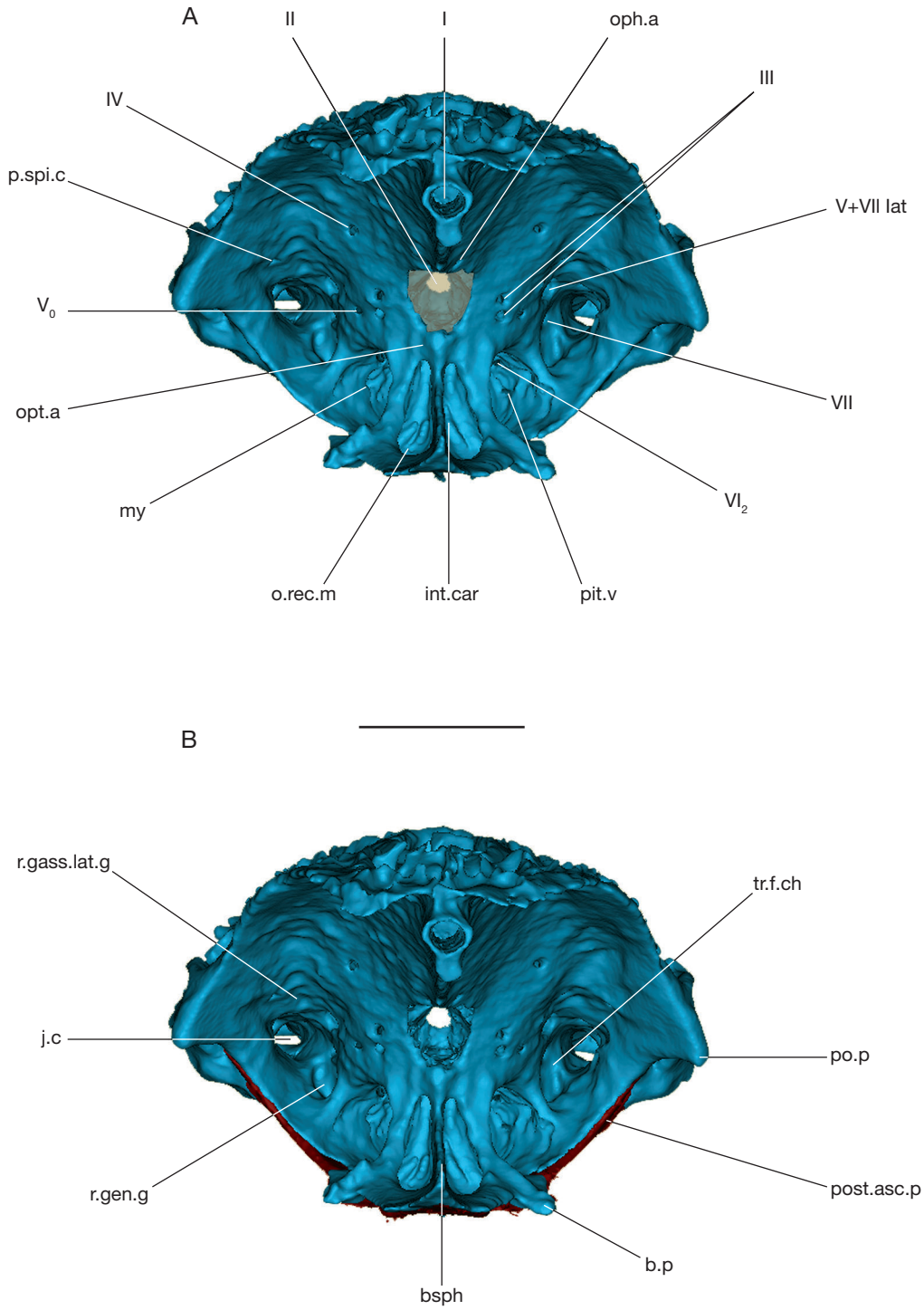

FIG. 4. — Surface rendering generated from CT Scan slices of AMNH FF 20852 in anterior view: **A**, braincase (**blue**); **B**, braincase and associated bones (parasphenoid in red). **Grey area**, not perichondrally lined surface. Abbreviations: see Material and methods. Scale bar: 5 mm.

orbitotemporal and the upper part of the otic regions are separated from the occipital arch and the lower part of the otic region by the otico-occipital fissure, the vestibular fontanelle and the ventral otic fissure. The braincase is tropibasic, with the orbit separated by a narrow interorbital septum and the endocranial cavity mainly situated dorsal to the septum. The skull is about 24 mm long, 16 mm wide at the level of the postorbital process, and 12 mm high at the level of the basipterygoid processes. This new braincase is thus slightly smaller than the previously described *Lawrenciella* braincases (Hamel & Poplin 2008).

Ethmoidal region. The ethmoidal region is largely missing anterior to the paired dorsal anterior myodomes (Fig. 2[d.ant.my]) for the superior oblique muscles. These depressions are dorsal to the canal for the olfactory nerves (Fig. 2[I]) and are separated by the incompletely ossified orbital septum (Fig. 2[iorb.s]).

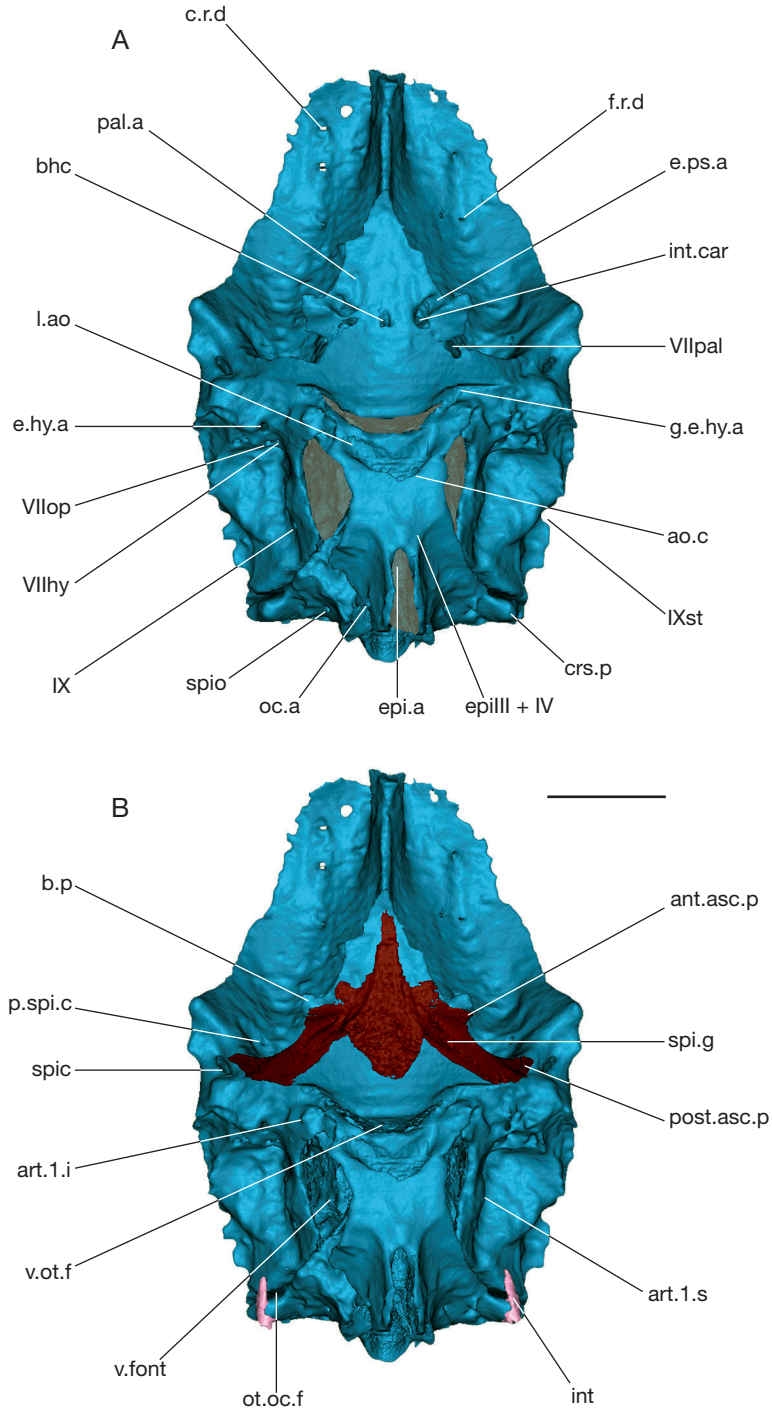

FIG. 5. — Surface rendering generated from CT Scan slices of the ventral surface of AMNH FF 20852: **A**, braincase (**blue**); **B**, braincase and associated bones (intercalar in **pink**; parasphenoid in **red**). **Grey area**, not perichondrally lined surface. Abbreviations: see Material and methods. Scale bar: 5 mm.

Orbitotemporal and upper part of the otic regions. The orbits are surrounded by a wide supraorbital shelf (Figs 2[s.s]; 3[s.s]) dorsally, which is confluent with a massive postorbital process (Figs 2[po.p]; 4[po.p]) posteriorly. The supraorbital shelf is pierced by several foramina for the passage of the ramus ophthalmicus superficialis, the ramus ophthalmicus lateralis and vessels (Figs 3[f.ram.dors]; 5[c.r.d, f.r.d]). The orbits are separated by the interorbital septum (Fig. 2[iorbs.s]) dorsally. The posterior part of the orbit shows a high pars basisphenoidea (Fig. 4[bsph]) that contains paired ventral depression for the right and left superior, inferior and internal recti muscles (Fig. 4[o.rec.m]). The base of the pars basisphenoidea is flanked by the basipterygoid process (Figs 2[b.p]; 4[b.p]; 5[b.p]). The anterior face of the pars basisphenoidea displays two vertical and parallel grooves for the internal carotid arteries (Fig. 4[int.car]). The optic

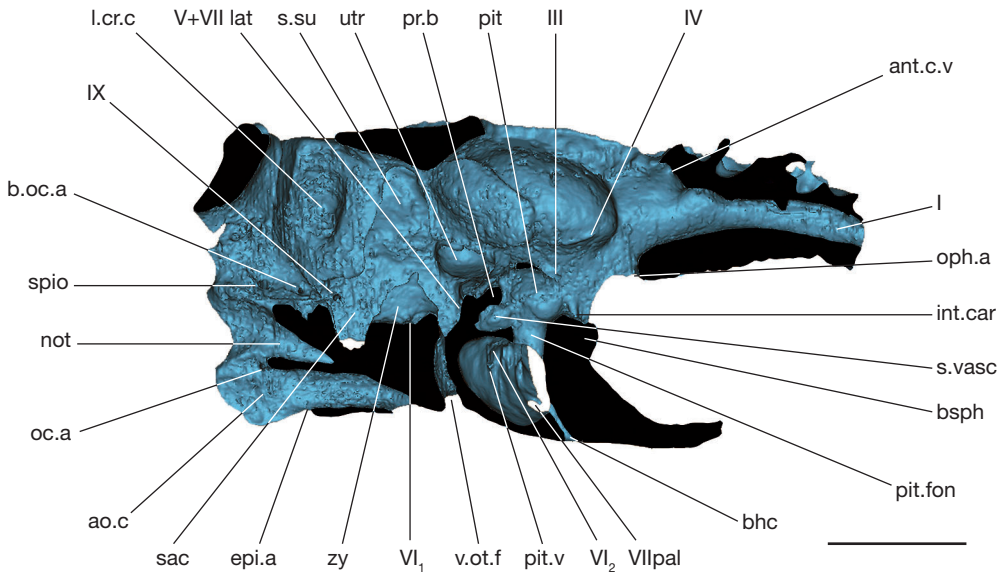

FIG. 6. — Surface rendering generated from CT Scan slices of the braincase (**blue**) of AMNH FF 20852 in sagittal view, left side. **Black area**, braincase section Abbreviations: see Material and methods. Scale bar: 5 mm.

arteries (Fig. 4[opt.a]) were in the grooves situated above the entrance of the internal carotids and below the optic nerve foramen (Fig. 4[II]) that pierces the braincase above the pars basisphenoidea. Flanking the optic foramen dorsolaterally are two small foramina for the ophthalmic artery (Fig. 4[oph.a]). Between the optic nerve foramen anteriorly and the trigeminofacialis chamber (Fig. 4[tr.f.ch]) posteriorly, lie a series of foramina that are, from anterior to posterior, the oculomotor nerve (Fig. 4[III]), the profundus nerve (Fig. 4[V_0]), the trigeminal and the lateralis trunk of the facial nerve (Fig. 4[V+VII lat]), and the facial nerve (Fig. 4[VII]). Dorsal and slightly anterior to the oculomotor foramina is the trochlear nerve exit (Fig. 4[IV]). The trigeminofacialis chamber is delimited by the orbital exit of the jugular vein (Fig. 4[j.c]), the gasserian and lateralis ganglia recess dorsally (Fig. 4[r.gass.lat.g]) and the geniculate ganglion recess ventrally (Fig. 4[r.gen.g]). A bridge separates the later recess to the deep, unpaired posterior myodome (Figs 2[my]; 6[my]) for the left and right external recti muscles. The posterior wall of the myodome is pierced by the foramen for the abducens nerve (Fig. 4[VI_2]). A deep groove that housed the pituitary vein (Figs 4[pit.v]; 6[pit.v]) lies below and in front of the abducens nerve. The roof of the myodome is fenestrated by a large pituitary fontanelle (Fig. 6[pit.fon]) that is confluent with a space for the saccus vasculosus (Fig. 6[s.vasc]) and the pituitary (Fig. 6[pit]) respectively. These recesses are bordered by the prootic bridge (Fig. 6[pr.b]) dorsoposteriorly. The latter is not continuous: an opening is present between the pituitary and the floor of the optic lobe. Behind the basipterygoid process, the lateral edge of the floor of the posterior myodome displays a pair of pronounced notches (Fig. 5[VIIpal]). Antero-medial to these lies the ventral opening of the bucco-hypophyseal canal (Fig. 5[bhc]) that runs upward and exits dorsally into the anterior part of the myodome.

In front of the anterior level of hyomandibular facet, the roof of the braincase displays an anteroposteriorly elongated anterior dorsal fontanelle (Fig. 3[ant.d.fon]) medially. The fontanelle ends anteriorly with a constriction indicating its epiphyseal part (Fig. 3[epi]). The anterior dorsal fontanelle is followed by a median ridge (Fig. 3[m.r]) anteriorly, and which is flanked by two paired lateral ridges of irregular shape (Fig. 3[l.r]). From the posterior border of the fontanelle, two prominent posterior dorsal crests (Fig. 3[cr.csp]) diverge until the otico-occipital fissure (Fig. 3[ot.oc.f]) and cover the path of the posterior semicircular canal. The otico-occipital fissure is confluent with the posterior dorsal fontanelle (Fig. 3[post.d.fon]), the anterior border of which being marked by an intrusive process (Fig. 3[l.st.a]). At approximately half length, the posterior dorsal crest is flanked by a large and deep posterior fossa bridgei (Fig. 3[p.fb]), which possesses intramural diverticuli (Fig. 8). A ridge covering the anterior semicircular canal diverges anteriorly from the medial edge of the posterior fossa bridgei until the anterior fossa bridgei (Fig. 3[a.fb]). The spiracular canal (Fig. 5[spic]) pierces the postorbital process vertically and exits dorsally through the anterior fossa and ventrally on the ventral surface of the postorbital process. In front of the anterior fossa and medial to the postorbital process lies another large pit, the prespiracular fossa (Fig. 3[p.spi.f]), the floor of which being pierced by a canal, maybe for an ophthalmic branch of the trigeminal or facial nerve (Figs 5[p.spi.c]; 8[p.spi.c]). The postorbital process is partly formed by a chondrified lateral commissure (Fig. 2[l.c]) that covers the jugular canal (Figs 4[j.c]; 7[j.c]) laterally. Posterior to the lateral commissure is an elongated and anteroventrally-directed articular facet for the hyomandibula (Fig. 2[f.hm]), below which lies the efferent hyoid artery foramen (Fig. 5[e.hy.a]; following Giles *et al.* 2015c for the interpretation of this foramen). Two openings for the hyomandibular (Figs 5[VIIhy]; 7[VIIhy]) and opercular (Figs 5[VIIop]; 7[VIIop]) branches of the facial

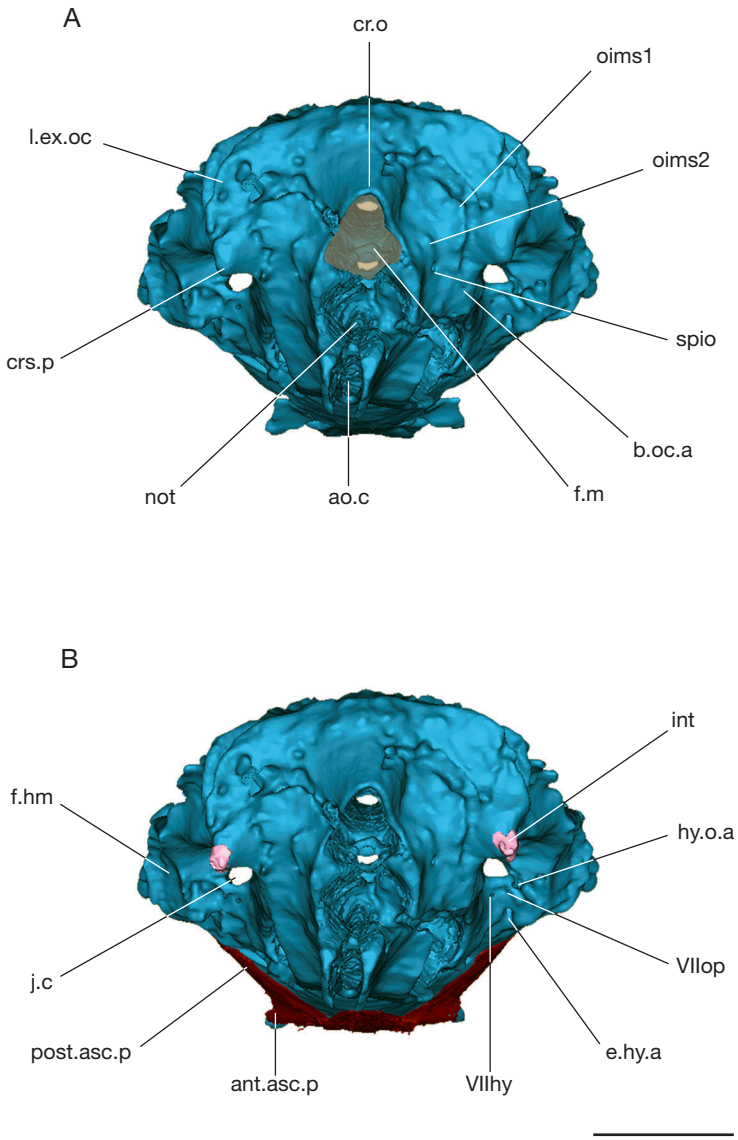

FIG. 7. — Surface rendering generated from CT Scan slices of AMNH FF 20852 in posterior view: **A**, braincase (**blue**); **B**, braincase and associated bones (intercalar in **pink**; parasphenoid in **red**). **Grey area**, not perichondrally lined surface. Abbreviations: see Material and methods. Scale bar: 5 mm.

nerve lie directly behind the hyomandibular articulation facet and below the posterior opening of the jugular canal. The hyo-opercular artery (Fig. 7[hy.o.a]) exits the jugular canal laterally via a foramen in the right side whereas it leaves only a groove extending outward from the posterior opening of the left jugular canal. The jugular vein probably lay in the jugular depression (Fig. 2[j.d]) that joins the posterior opening of the jugular canal to the vagus nerve exit (Fig. 2[X]), which forms a wider area of the otico-occipital fissure. Anteroventral to the vagus nerve exit, the lateral wall of the braincase is pierced by the glossopharyngeal nerve (Fig. 2[IX]) foramen, which is followed by a groove on the horizontal semicircular canal ridge for its supratemporal branch (Fig. 2[IXst]) that might ran in a notch on the lateral edge of the dorsal surface of the braincase (Fig. 3[IXst]).

Between the glossopharyngeal foramen and the vestibular fontanelle (Fig. 2[v.font]), which is continuous with the otico-occipital fissure, is an articular facet for the first suprapharyngobranchial (Fig. 2[art.1.s]; 5[art.1.s]). The vestibular fontanelle is separated from the ventral otic fissure (Fig. 2[v.ot.f]; 5[v.ot.f]; 6[v.ot.f]) by a bony bridge. Immediately behind the fissure, the aortic canal (Figs 5[ao.c]; 6[ao.c]; 7[ao.c]) exits and divides into paired grooves for the lateral aortae (Fig. 5[l.ao]). Each lateral aorta gave off the efferent hyoid artery (Fig. 5[g.e.hy.a, e.hy.a]) that bends outward and backward in front of the articular facet for the first infrapharyngobranchial (Fig. 5[art.1.i]), and the internal carotid artery that ran forward until the level of the bucco-hypophyseal ventral opening where it enters the floor of the braincase (Fig. 5[int.car]). Before penetrating the endocranium, the internal carotid artery gave off the efferent pseudobranchial artery (Fig. 5[e.ps.a]), which is housed in an anteriorly divergent deep groove, and the palatine artery (Fig. 5[pal.a]) that extended in a shallow anterior groove. More posteriorly, a large foramen marks the

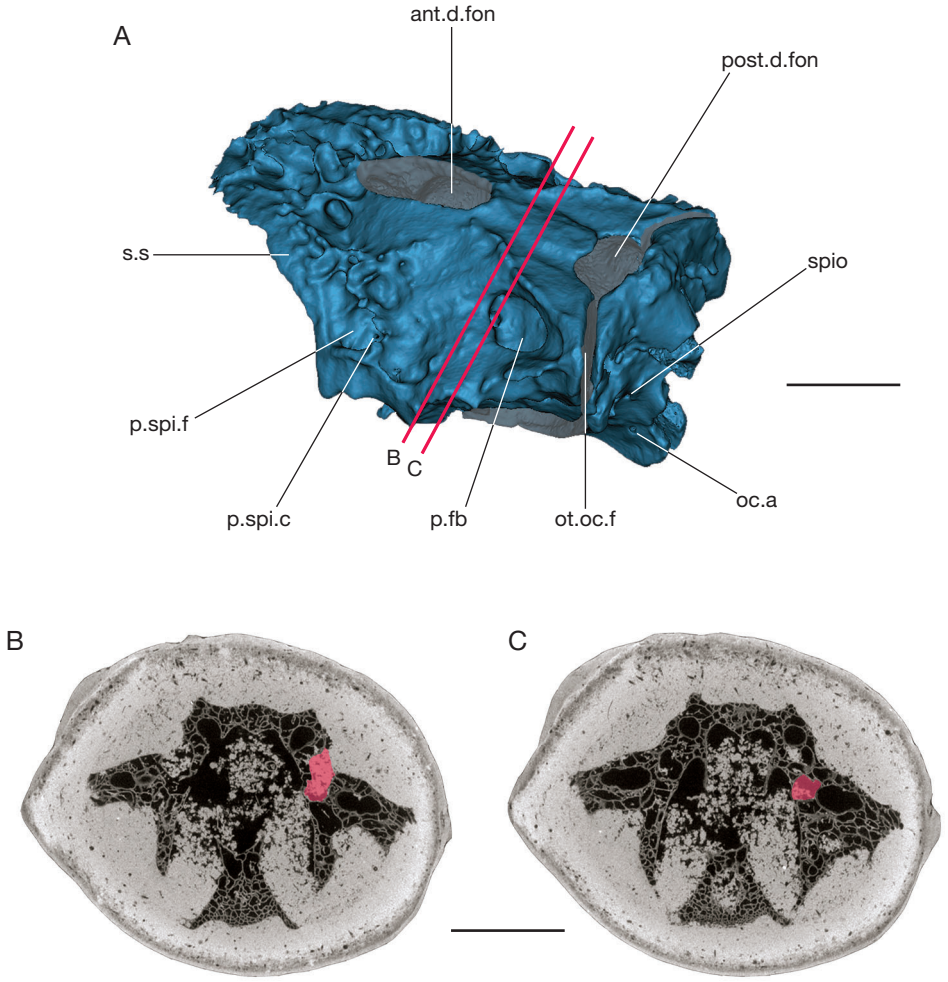

FIG. 8. — Surface rendering generated from CT Scan slices of AMNH FF 20852: **A**, postero-lateral view of the braincase (**blue**); the transverse microtomographic slices of B and C are indicated in red line. The **red colored area** of the braincase in B and C represent the intramural diverticuli of the posterior fossa bridgei. Abbreviations: see Material and methods. Scale bars: 5 mm.

divergence between the dorsal aorta, which is housed into the aortic canal, and the epibranchial arteries (Fig. 5[epi.a]). Anterior to this foramen are paired anteriorly divergent grooves probably for a common root of the epibranchial arteries III and IV (Fig. 5[epi III + IV]).

Occipital region. In the posterior view, the occiput possesses three openings that are, from dorsal to ventral, for the foramen magnum (Fig. 7[f.m]), the notochordal canal (Fig. 7[not]), and the aortic canal (Fig. 7[ao.c]) respectively. The floor of the aortic canal is not complete posteriorly behind the foramen for the epibranchial arteries, probably due to preservation artefact. Above the foramen magnum lies a rather low median occipital crest (Fig. 7[cr.o]). The dorsolateral edge of the occipital unit displays a pair of dorsolateral processes (Fig. 7[l.ex.oc]) and a pair of cranio-spinal processes (Figs 2[crs.p]; 5[crs.p]; 7[crs.p]), which bear the intercalar bones (Figs 2[int]; 5[int]; 7[int]). Although the posterior wall of the occipital ossification is damaged, it shows two pair of ridges (Fig. 7[oims1, oism2]) for the insertion of the first and second inter muscular septa. The foramina for the spino-occipital nerve (Figs 5[spio]; 6[spio]; 7[spio]; 8[spio]) lies at the base of the smallest of these two ridges, the medial ones (Fig. 7[oism2]). At the base of the lateral ridges (Fig. 7[oism1]) is a small foramen, probably for a branch of the occipital artery (Figs 6[b.oc.a]; 7[b.oc.a]). At the level of the roof of the aortic canal, are the foramina for the occipital artery (Figs 5[oc.a]; 6[oc.a]; 8[oc.a]).

Internally is located a medial ossification, the zygal plates (Fig. 6[zy]) formed by two thin and triangular blades covering laterally the anterior end of the notochordal canal. Each blade displays a small foramen for the abducens nerve (Fig. 6[VI_1]) at their medial wall.

Intercalar. Posterior and lateral to the vagus foramen, on the lateral edge of the occipital region, at the same level as the floor of the foramen magnum, paired intercalar bones (Figs 2B[int]; 5B[int]; 7B[int]; 9[int]) are tightly attached to the cranio-spinal processes of the neurocranium. Their internal edges show a concavity posteriorly that surrounds the cranio-spinal process posterolaterally. The intercalar bones then taper and project anteriorly to cover the metotic fissure, but they do not extend farther than the anterior edge

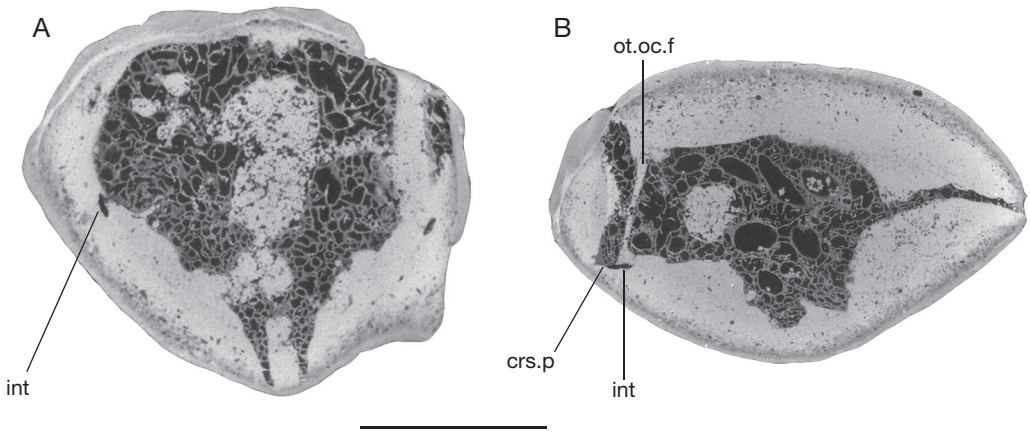

FIG. 9. — Microtomographic slices through the intercalars of AMNH FF 20852: **A**, cross section; **B**, saggital section through the left intercalar. Abbreviations: see Material and methods. Scale bar: 5 mm.

of the fissure and the vagus foramen. Cranio-spinal processes are also present in the *Lawrenciella* specimen described by Hamel & Poplin (2008), but they do not project anteriorly. The intercalar bones of the specimen studied here are not spongious (Fig. 9), unlike the endochondral bone of the neurocranium. These observations suggest that these anterior projections represent distinct bones that are not endochondral ossifications of the neurocranium, but rather independent bones that are tightly associated with the cranio-spinal processes of the braincase. It is however not possible to say whether these intercalars are membranous bones as in *Amia*, teleosts, Mesozoic caturids, pholidophorids and leptolepids.

Parasphenoid. The parasphenoid seems to be not entirely preserved, but still appears tightly attached to the ventral face of the endocranium. The CT scan images show numerous small denticles on the ventral surface of the parasphenoid. The latter extends and tapers anteriorly until the level of the mid-orbit, though it seems that its anterior end is missing. The preserved part of the posterior edge is rounded and does not reach the ventral otic fissure posteriorly. The parasphenoid covers the internal carotids and the palatine branches of the facial nerves. The anterior ascending processes (Fig. 5[ant.asc.p]) cover the base of the endocranial basipterygoid processes. Their anterior margin of the dorsal surface displays a short groove medially for the passage of the efferent pseudobranchial artery (Fig. 5[e.ps.a]). The posterior ascending processes (Figs 2[post.asc.p]; 4[post.asc.p]; 5[post.asc.p]) extend dorsally almost as far as the lateral commissure and terminate at the level of the spiracular canals. Two deep spiracular grooves (Fig. 5[spi.g]) extend along the posterior ascending processes. On the dorsal surface of the parasphenoid is a small bump located at the level of the opening of the bucco-hypophyseal canal.

Endocast anatomy. The telencephalon (Fig. 10[tel]) is small and slightly narrower than the paired olfactory bulbs (Fig. 10[olf.b]) in front. The olfactory bulbs extends forward as a long unpaired olfactory canal (Figs 10[I]; 11[I]; 12[I]), which is not preserved more anteriorly. A canal for the anterior cerebral (Figs 10[ant.c.v]; 11[ant.c.v]; 12[ant.c.v]) vein originates on the roof of the telencephalon and extends anterolateroventrally to reach the left orbit in front of the trochlear nerve foramen.

The dorsal part of the diencephalon (Fig. 10[die]) is very short and restricted to the area beneath the epiphyseal part of the anterior dorsal fontanelle (Fig. 10[epi]). Its floor comprises from dorsal to ventral respectively: paired canals for the small ophthalmic arteries (Figs 11[oph.a]; 12[oph.a]), a single, large optic nerve foramen (Figs 11[II]; 12[II]), paired internal carotid canals (Figs 11[int.car]; 12[int.car]), a large hypophyseal recess (Fig. 12[pit]), which opens in the roof of the posterior myodome via the pituitary fontanelle (Fig. 11[pit.fon]) and which extends backward with the saccus vasculus (Figs 11[s.vasc]; 12[s.vasc]).

The anterior dorsal fontanelle communicates ventrally with two large optic lobes (Figs 10[opt.l]; 12[opt.l]) of the mesencephalic region. The floor of the optic lobes is pierced by the trochlear (Figs 11[IV]; 12[IV]) and oculomotor (Figs 11[III]; 12[III]) canals, the latter flanking the hypophyseal recess.

The metencephalic region is mainly represented by paired, anteriorly divergent, large cerebellar auricles (Figs 10[aur]; 12[aur]). There is an antero-posterior ridge for the longitudinal dorsal vein (Fig. 10[l.d.v]) between the cerebellar auricles. The middle cerebral vein (Figs 10[md.c.v]; 11[md.c.v]) forms a ridge along the anterodorsal part of the cerebellar auricles that extends downward. Three canals for the profundus (Figs 11[V_0]; 12[V_0]), trigeminal and lateralis (V + VII lat) and facial (VII) emerge between the floor of the cerebellar auricles and the utricular recess. The abducens nerve (Figs 11[VI_2]; 12[VI_2]) pierced the floor of the metencephalic region between the two saccular chambers (Fig. 12[sac]).

Behind the cerebellar auricles is a slight and smooth swelling that might represent the area octavolateralis of the rhombencephalon (Fig. 10[a.octl]) rather than a cerebellar corpus because the latter is anterior to the cerebellar auricles

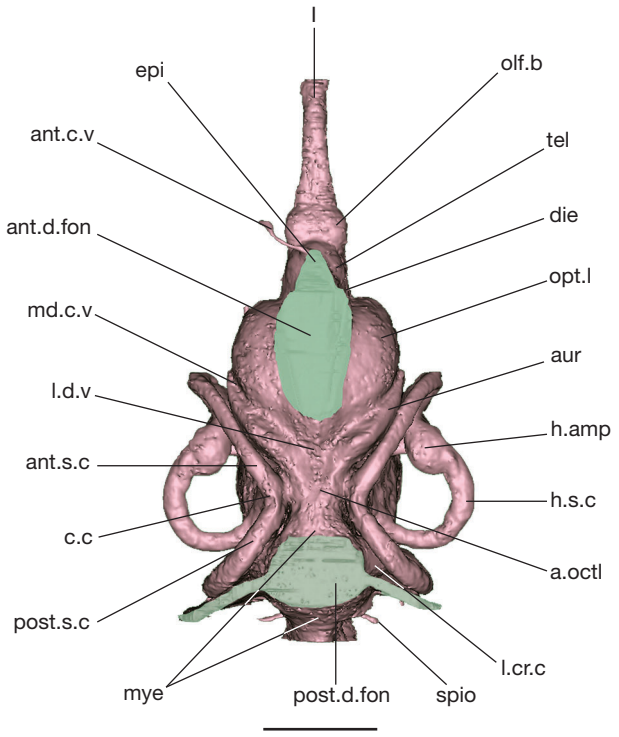

Fig. 10. — Surface rendering generated from CT Scan slices of the dorsal surface of the endocranial cavity (**pink**) of AMNH FF 20852. **Grey area**, cast section. Abbreviations: see Material and methods. Scale bar: 5 mm.

in recent sharks and actinopterygians. This area then widens backward until the posterior dorsal fontanelle. A small intramural pocket that represent the lateral cranial canal (Figs 10[l.cr.c]; 12[l.cr.c]) projects through the loop of the posterior semicircular canal. In front of the otico-occipital fissure, the lateral cranial canal communicates posteriorly with the myelencephalic cavity (Fig. 12[mye]).

Two canals open on each side of the inner wall of the foramen magnum: the spino-occipital nerve canal (Figs 10[spio]; 11[spio]; 12[spio]) posteriorly and the canal for a branch of the occipital artery (Fig. 11[b.oc.a]). Then the foramen magnum extends anteriorly as the endocranial cavity. An occipital artery canal (Figs 11[oc.a]; 12[oc.a]) opens on the wall of the aortic canal, which remains unpaired, but is enlarged anteriorly as it opens into two deep and divergent grooves for the lateral aorta. The notochord canal (Fig. 12[not]) tapers anteriorly and does not reach the ventral otic fissure.

The inner ear comprises three semicircular canals: the horizontal (Figs 10[h.s.c]; 12[h.s.c]), the posterior (Figs 10[post.s.c]; 12[post.s.c]) and the anterior (Figs 10[ant.s.c]; 12[ant.s.c]). The two latter semicircular canals meet dorsally at a crus commune (Fig. 10[c.c]) that extends downward as a sinus superior (Fig. 12[s.su]), which communicates with the saccular chamber (Fig. 12[sac]) and the utricular recess (Figs 7[utr]; 12[utr]). The horizontal ampullae (Figs 10[h.amp]; 12[h.amp]) is situated at the antero-dorsal corner of the saccular chamber, just behind the anterior ampullae (Fig. 12[ant.amp]), while the posterior ampullae (Fig. 12[post.amp]) is at the postero-dorsal corner of the saccular chamber. No otoliths are preserved.

DISCUSSION

Difference between *Lawrenciella schaefferi* and this specimen (*Lawrenciella* sp.)

Differences between *Lawrenciella* sp. and *Lawrenciella schaefferi* are either due to preservational artefacts, or to intraspecific and/or intrageneric diversity. Intraspecific and intrageneric variability is hard to evaluate in Paleozoic fishes because each species is usually represented by only very few numbers of specimens. This variability questions the validity and the phylogenetic status of some of the morphological characters that might be used to resolve deep nodes.

The smaller size of the specimen studied here compared to *Lawrenciella schaefferi* and the lack of most of its ethmoid region, which is one the latest part of the braincase to ossify, might illustrate a younger age of the specimen studied here. It is known that individual variability may depend on the age of the specimen in « paleonisformes » (e.g., the number of ossification in *Pteronisculus magnus* Nielsen, 1942; the shape and position of the communication between the fossa bridgei and the intramural space, the completeness of the continuum of the otico-occipital fissure and posterior dorsal fontanelle, the presence of the ventral otic fissure in *Boreosomus piveteaui* Nielsen, 1942; the length of the anterior dorsal fontanelle in the genera *Boreosomus* Véran, 1971). In the specimen studied here, the anterior dorsal fontanelle (ant.d.fon) is slightly more elongated anteriorly than in *Lawrenciella schaefferi*, extending a bit further than the level of the postorbital process, and covering most of the telencephalon.

Examples of intraspecific and intrageneric diversity that is probably not age dependent are also known: the eye muscle attachment in *Australosomus kochi* Stensiö, 1932 (Nielsen 1949); the extent of the bony edge of the anterior fossa bridgei in the genus *Boreosomus* (Véran 1971), the course of the profundus nerve in *Kansasiella* (Poplin 1974); the course of the facial and trigeminal nerves in *Pteronisculus stensioi* White, 1933, (Nielsen 1942); the canal and foramina for the ophthalmic branches of the trigeminal nerve in *Kansasiella* Poplin, 1974, *Pteronisculus magnus* (Nielsen 1942) and *Boreosomus* (Nielsen 1942; Lehman 1952); the course of the hyomandibular and opercular branches of the facial nerve and the hyo-opercular artery relative to the jugular canal in *Kansasiella* (Poplin 1974).

Below is a list of other minor differences between the braincase of *L. schaefferi* and that of *L.* sp., which may either be intraspecifc variation, or suggest the presence of distinct species:
– The process that overhangs the anterior border of the posterior dorsal fontanelle has a different shape: it tapers anteriorly in the specimen studied here whereas it flares anteriorly in *Lawrenciella schaefferi*;
– The floor of the pre-spiracular fossa is pierced by a canal in *Lawrenciella* sp., maybe for an ophthalmic branch of the trigeminal or facial nerve (p.spi.c). No such canal is present in *Lawrenciella schaefferi*;
– In *Lawrenciella* sp., behind the basipterygoid process, on the floor of the posterior myodome there is no foramen for the palatine branches of the facial nerve but instead a large notch on the edge of the floor;

– There is no evidence of a foramen for the supra temporal branch of the glossopharyngeal nerve on the dorsal surface of the braincase, lateral to the posterior fossa bridgei in *Lawrenciella* sp.. However a deep notch located at the same level might have housed this nerve (IXst);
– There is no median recess of the occipital ossification overhanging the posterior dorsal fontanelle anteriorly in *Lawrenciella* sp.;
– The presence of posterior fossa bridgei with intramural diverticuli (Fig. 8);
– No intracranial ossicles covering the diencephalic and mesencephalic region laterally and in front of the optic foramen;
– The prootic bridge is not continuous: an opening is present between the pituitary and the floor of the optic lobes;
– The parasphenoid does not reach the ventral otic fissure posteriorly.

Finally, the features that are missing because of preservation artefacts are:
– In *Lawrenciella* sp., the floor of the aortic canal is not complete posteriorly behind the foramen for the epibranchial arteries. The floor of the canal reaches the edge of the nodule at this level, so that some parts might be not completely preserved;
– The lack of intercalars in *Lawrenciella schaefferi* might be a preservation artefact since other dermal or membranous are not associated to the already known specimens, except some bit of parasphenoids in few specimens (Hamel & Poplin 2008);
– The ethmoid part that is supposed to contain a single median anterior myodome for ocular muscles is not preserved in the specimen studied here;
– The fact that the parasphenoid does not reach the ventral otic fissure posteriorly in *Lawrenciella* sp. might be a preservation artefact.

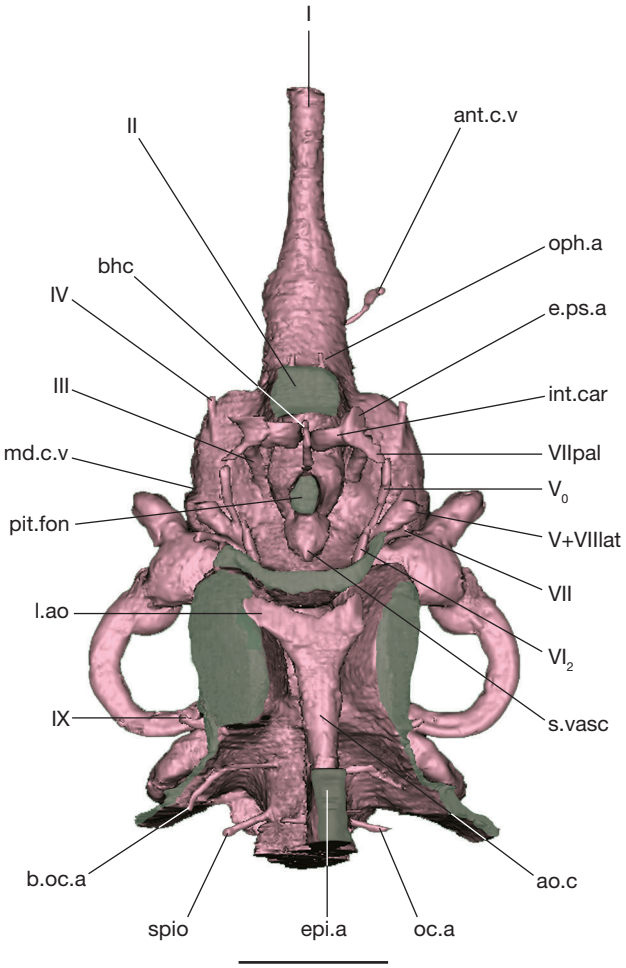

Fig. 11. — Surface rendering generated from CT Scan slices of the ventral surface of the endocranial cavity (**pink**) of AMNH FF 20852. **Grey area**, cast section. Abbreviations: see Material and methods. Scale bar: 5 mm.

Phylogenetic position

The phylogenetic relationships of *Lawrenciella* are still under consideration. It was first interpreted as a member of the order Palaeonisciformes. However, this group is resolved as paraphyletic in all recent cladistic studies (Coates 1999; Hamel 2007; Giles *et al.* 2015a, b). Analyses of neurocranial characters alone were not satisfactory to determine the precise phylogenetic position of *Lawrenciella* within the early actinopterygians: it is resolved as a stem actinopterygian (Hamel 2007), an actinopteran (Poplin 1984; Hamel & Poplin 2008), or a stem neopterygian together with some other « palaeonisciforms » from the Upper Carboniferous (e.g., *Coccocephalus* Watson, 1925, *Kansasiella*, *Mesopoma* Traquair, 1890) (Hamel & Poplin 2008). However, the neurocranial characters shared by *Lawrenciella,* and those forms are all homoplasic (Hamel & Poplin 2008). The characters belonging to the dermal bones might help in resolving the phylogenetic position of *Lawrenciella*. However, only the parasphenoid was known before the present study. Consequently, adding *Lawrenciella* in a broad phylogenetic analysis including both endocranial and dermal features might be problematic given the very large quantity of missing data.

The parasphenoid of *Lawrenciella schaefferi* is crown-group actinopteran-like in extending posteriorly to reach the ventral otic fissure without covering it (Coates 1999). As discussed earlier, the parasphenoid of *Lawrenciella* sp. does not reach the ventral fissure. Consequently, either the parasphenoid of the latter is not fully preserved posteriorly, or the posterior extent of the parasphenoid is more polymorphic than thought, hence, calling into question its phylogenetic status and use in data matrices.

The intercalar bones among actinopterygians

In living actinopterygians, the intercalar is only present in *Amia* and teleosts as a membrane bone. It is situated posterolateral to the vagus nerve and it spreads anteriorly, over the posterior and lateral surfaces of the otic region. It gives origin to the ligament from the ventral process of the dermal post-temporal (Patterson 1973).

In some early holosteans and teleosteans, such as the Mesozoic caturids, pholidophorids and leptolepids, the intercalar had an endochondral core from which membranous outgrowths developed (Schaeffer 1971; Patterson 1975). Furthermore, the endochondral core of the intercalar of the pholidophorids is said to develop in the cranio-spinal process of the braincase (Patterson 1975).

The cranio-spinal process is homologous to that of the extant chondrosteans because, in the latter, the cranio-spinal process receives the ligament from the ventral limb of the post-temporal

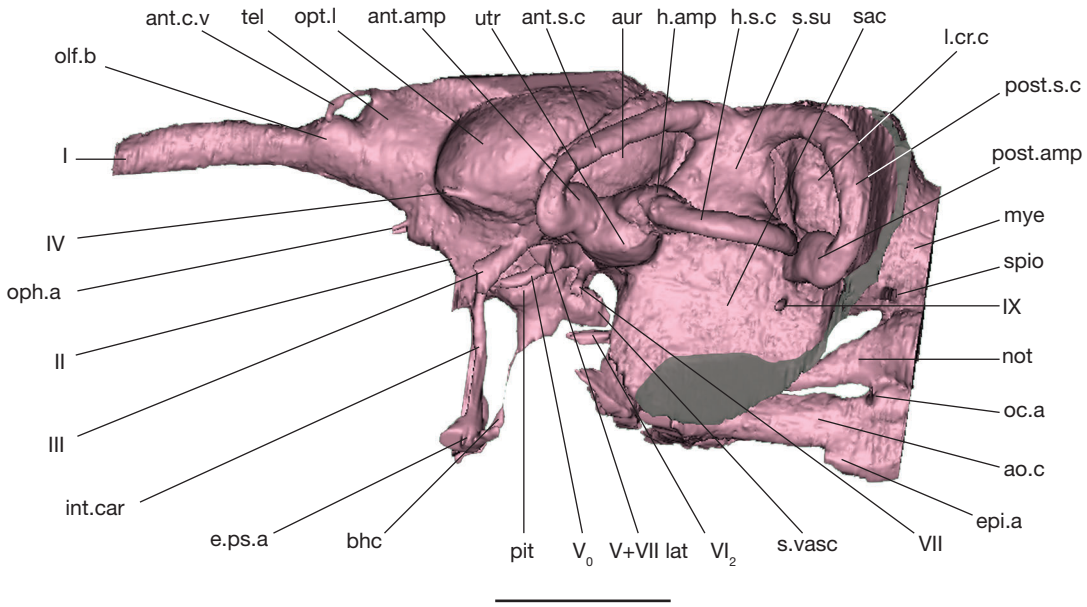

FIG. 12. — Surface rendering generated from CT Scan slices of the left lateral surface of the endocranial cavity (**pink**) of AMNH FF 20852. **Grey area**, cast section. Abbreviations: see Material and methods. Scale bar: 5 mm.

(Patterson 1975). This led Gardiner (1984) to assume that the cranio-spinal process of *Mimipiscis* Gardiner & Bartram, 1977 and other "palaeoniscids" is actually made up by the intercalar. This would imply that the intercalar is primitively present in osteichthyans, since a cranio-spinal process was recently resolved as a synapomorphy of the crown group gnathostomes, plus *Janusiscus* Giles, Friedman & Brazeau, 2015 and *Ramirosuarezia* Pradel, Maisey, Tafforeau & Janvier, 2009 (Giles *et al.* 2015a). In Paleozoic actinopterygians, the cranio-spinal process is part of the endochondral braincase. Consequently, one can suggest that the intercalar is primitively endochondral in origin, and forms the cranio-spinal process of Paleozoic actinopterygians. Extensive outgrowths of membrane bone from this endochondral core would then represent an advanced feature of neopterygians. The lack of the endochondral part would be a characteristic of *Amia* and modern teleosts independently, as already suggested by Patterson (1975).

Lawrenciella schaefferi possesses endochondral cranio-spinal processes, as *Lawrenciella* sp. The latter displays in addition an anteriorly directed outgrowth from this process that is not present in *Lawrenciella schaefferi*. From these observations, we suggest that the intercalar of the *Lawrenciella* specimen studied here is actually made up by an endochondral core (the cranio-spinal press) that is present also in *Lawrenciella schaefferi*, plus an anteriorly directed outgrowth. Further analyses are needed in order to test whether this outgrowth is actually made of membranous tissue as in neopterygians. If the intercalar of *Lawrenciella* sp. actually have a membranous origin, this might resolve *Lawrenciella* as at least a neopterygian, more advanced than other "palaeoniscoids" that do not possess the outgrowth of the intercalar, but less advanced than crown halecomorphs and teleosteans that have lost the endochondral part.

In pholidophorids, there is no posterior dorsal fontanelle. In primitive forms, the otico-occipital fissure is continuous ventro-dorsally and part of the fissure around the vagus nerve is covered superficially by membranous outgrowths of the intercalar (Patterson 1975). Also, in some pholidophorids, the epioccipital has also developed membranous outgrowths that overlap the dorso-lateral part of the fissure.

In *Lawrenciella,* the otico-occipital fissure is complete from the vestibular fontanelle to the posterior dorsal fontanelle, there is no such epioccipital extension, but the anterior extension of the intercalar covers the fissure around the vagus as in pholidophorids. These observations suggest that *Lawrenciella* shows an intermediate anatomical condition between forms such as *Mimipiscis* (only endochondral intercalar - the spino-occipital process - that does not cover the complete otico-occipital fissure extending from the vestibular fontanelle to the posterior dorsal fontanelle) and pholidophorids (intercalar made up by endochondral and membranous outgrowths that cover an incomplete otico-occipital fissure that is partially closed).

The forward extension of occipital bones over the otic region is one of the three processes that are involved in the closure of the actinopterygian otico-occipital fissure; the two other processes being the closure in cartilage during ontogeny by ventral and dorsal commissures (De Beer 1937; Patterson 1975). *Lawrenciella* does not show any evidence of commissures, nor suture between the occipital arch and the otic region. It only possesses superficial overlapping of the fissure by the intercalar anteriorly directed extension. This would suggest that *Lawrenciella* is actually showing the first step of the closure of the otico-occipital fissure in actinoptyerygians, which preceeded phylogenetically the other processes of closure (commissures, suture and anteriorly extension of the other occipital bones). In modern teleosts, the loss of the endochondral part of the intercalar would be the consequence of the closure of the supravagal part of the cranial fissure and forward extension of the exoccipital above the vagus canal (Patterson 1975).

Acknowledgements
We thank Philippe Janvier (Muséum national d'Histoire naturelle, Paris), Nalani Schnell (MNHN) and Gloria Arratia (University of Kansas, Lawrence, USA) for their discussion and help, and the staff at the Microscopy and Imaging Facility of the AMNH. The main work was supported by the ATM Emergence grant (MNHN) and by the H. R. & E. Axelrod Research Chair in paleoichthyology (AMNH).

REFERENCES

Coates M. I. 1999. — Endocranial preservation of a Carboniferous actinopterygian from Lancashire, UK, and the interrelationships of primitive actinopterygians. *Philosophical Transactions of the Royal Society of London, B* 354: 433-462. http://dx.doi.org/10.1098/rstb.1999.0396

De Beer G. R. 1937. — *The Development of the Vertebrate Skull*. Oxford University Press, Oxford, 552 p.

Dupret V., Sanchez S., Goujet D., Tafforeau P. & Ahlberg P. E. 2014. — A primitive placoderm sheds light on the origin of the jawed vertebrate face. *Nature* 507 (7493): 500-503. http://dx.doi.org/10.1038/nature12980

Faircloth B. C., Sorenson L., Santini F. & Alfaro M. E. 2013. — A phylogenomic perspective on the radiation of ray-finned fishes based upon targeted sequencing of ultraconserved elements (UCEs). *PLoS ONE* 8 (6): e65923. http://dx.doi.org/10.1371/journal.pone.0065923

Gardiner B. G. 1984. — The relationships of the palaeoniscid fishes, a review based on new specimens of *Mimia* and *Moythomasia* from the Upper Devonian of Western Australia. *Bulletin of the British Museum (Natural History). Geology* 37:173-428.

Gardiner B. G., Maisey J. G. & Littlewood D. T. J. 1996. — Interrelationships of basal neopterygians, *in* Stiassny M., Parenti L. & Johnson G. D. (eds.), *Interrelationships of Fishes*. Academic Press, NewYork, 29 p.

Giles S. & Friedman M. 2014. — Virtual reconstruction of endocast anatomy in early ray-finned fishes (Osteichthyes, Actinopterygii). *Journal of Paleontology* 88 (4): 636-651. http://dx.doi.org/10.1666/13-094

Giles S., Friedman M., & Brazeau M. D. 2015a. — Osteichthyan-like cranial conditions in an Early Devonian stem gnathostome. *Nature* 520 (7545): 82-85. http://dx.doi.org/10.1038/nature14065

Giles S., Darras L., Clément G., Blieck A. & Friedman M. 2015b. — An exceptionally preserved Late Devonian actinopterygian provides a new model for primitive cranial anatomy in ray-finned fishes. *Proceeding of the Royal Society of London B,* 282 (1816): 20151485. http://dx.doi.org/10.1098/rspb.2015.1485

Giles S., Coates M. I., Garwood R. J., Brazeau M. D., Atwood R., Johanson Z., & Friedman M. 2015c. — Endoskeletal structure in *Cheirolepis* (Osteichthyes, Actinopterygii), An early ray-finned fish. *Palaeontology* 58 (5): 849-870. http://dx.doi.org/10.1111/pala.12182

Grande L. 2010. — An empirical synthetic pattern study of gars (Lepisosteiformes) and closely related species, based mostly on skeletal anatomy. The resurrection of Holostei. *American Society of Ichthyologists and Herpetologists Special Publication. Supplementary issue of Copeia* 10 (2A): 1-871.

Hamel M. H. 2007. — *Étude morpho-anatomique approfondie de l'endocrâne d'actinoptérygiens du Carbonifère supérieur du Kansas et recherches du message phylogénétique des caractères de l'endocrâne des actinoptérygiens basaux.* PhD dissertation, Muséum National d'Histoire Naturelle, Paris, 194 p.

Hamel M. H. & Poplin C. 2008. — The braincase anatomy of *Lawrenciella schaefferi*, actinopterygian from the Upper Carboniferous of Kansas (USA). *Journal of Vertebrate Paleontology* 28 (4): 989-1006. http://dx.doi.org/10.1671/0272-4634-28.4.989

Lane J. A. 2010. — Morphology of the braincase in the Cretaceous hybodont shark *Tribodus limae* (Chondrichthyes: Elasmobranchii), based on CT Scanning. *American Museum Novitates* 3681: 1-70. http://dx.doi.org/10.1206/681.1

Lehman J. P. 1952. — Étude complémentaire des poissons de l'Éotrias de Madagascar. *Kunglige Svenska Vetenskapsakademiens Handligar, 4th Ser* 2 (6): 1-201.

Maisey J. G. 2005. — Braincase of the Upper Devonian shark *Cladodoides wildungensis* (Chondrichthyes, Elasmobranchii), with observations on the braincase in early chondrichthyans. *Bulletin of the American Museum of Natural History* 288: 1-103. http://dx.doi.org/10.1206/0003-0090(2005)288<0001:BOTUDS>2.0.CO;2

Maisey J. G. 2007. — The braincase in Paleozoic symmoriiform and cladoselachian sharks. *Bulletin of the American Museum of Natural History* 307: 1-122. http://dx.doi.org/10.1206/0003-0090(2007)307[1:TBIPSA]2.0.CO;2

Maisey J. G. & Lane J. A. 2010. — Labyrinth morphology and the evolution of lowfrequency phonoreception in elasmobranchs. *Comptes Rendus Palevol* 9 (2010): 289-309. http://dx.doi.org/10.1016/j.crpv.2010.07.021

Nielsen E. 1942. — *Studies on Triassic Fishes from East Greenland. I.* Glaucolepis *and* Boreosomus. Palaeozoologica Groenlandica, 403 p.

Nielsen E. 1949. — *Studies on Triassic fishes from East Greenland II.* Australosomus *and* Birgeria. Palaeozoologica Groenlandica, 309 p.

Patterson C. 1973. — The interrelationships of Holosteans, *in* Greenwood P. H., Miles R. S. & Patterson C. (eds), *Interrelationships of Fishes*. *Zoological Journal of the Linnean Society of London* 53 (suppl. 1): 233-305.

Patterson C. 1975. — The braincase of pholidophorid and leptolepid fishes, with a review of the actinopterygian braincase. *Philosophical Transactions of the Royal Society of London, B* 269: 275-579.

Poplin C. 1974. — Étude de quelques paléoniscidés pennsylvaniens du Kansas. CNRS, Paris, 151 p. (*Cahiers de Paléontologie*).

Poplin C. 1984. — *Lawrenciella schaefferi* n.g., n.sp. (Pisces: Actinopterygii) and the use of endocranial characters in the classification of the Palaeonisciformes. *Journal of Vertebrate Paleontology* 4 (3): 413-421. http://dx.doi.org/10.1080/02724634.1984.10012019

Pradel A., Langer M., Maisey J. G., Geffard-Kuriyama D., Cloetens P., Janvier P. & Tafforeau P. 2009a. — Skull and brain of a 300 million-year-old chimaeroid fish revealed by synchrotron holotomography. *Proceedings of the National Academy of Science of the United Stateds of America*. 106 (13): 5224-5228. http://dx.doi.org/10.1073/pnas.0807047106

Pradel A., Maisey J. G., Tafforeau P. & Janvier P. 2009b. — An enigmatic gnathostome vertebrate skull from the Middle Devonian of Bolivia. *Acta Zoologica* 90 (s1): 123-133. http://dx.doi.org/10.1111/j.1463-6395.2008.00350.x

Pradel A. 2010. — Skull and brain anatomy of Late Carboniferous Sibyrhynchidae (Chondrichthyes, Iniopterygia) from Kansas and Oklahoma (USA). *Geodiversitas* 32 (4): 595-661. http://dx.doi.org/10.5252/g2010n4a2

Pradel A., Tafforeau P., Maisey J. G. & Janvier P. 2011. — A new Paleozoic Symmoriiformes (Chondrichthyes) from the Late Carboniferous of Kansas (USA) and cladistic analysis of early chondrichthyans. *PLoS ONE* 6: e24938. http://dx.doi.org/10.1371/journal.pone.0024938

Pradel A., Maisey J. G., Tafforeau P., Mapes R. H. & Mallatt J. 2014. — A Palaeozoic shark with osteichthyan-like branchial arches. *Nature* 509 (7502): 608-611. http://dx.doi.org/10.1038/nature13195

Sallan L. C. 2014. — Major issues in the origins of ray-finned

fish (Actinopterygii) biodiversity. *Biological Reviews* 89(4), 950-971. http://dx.doi.org/10.1111/brv.12086

SCHAEFFER B. 1971. — The braincase of the holostean fish *Macrepistius*, with comments on neurocranial ossiffcation in the Actinopterygii. *American Museum Novitates* 2459: 1-34.

VÉRAN M. 1971. — *Étude complémentaire de* Boreosomus reuterskiöldi *et de* Boreosomus arcticus*, poissons de l'Éotrias du Spitsberg*. PhD dissertation, Faculté des Sciences de Paris, 79 p.

Submitted on 26 January 2016;
accepted on 18 August 2016;
published on 30 December 2016.